1-2019

Shear Lag Factors for Tension Angles with Unequal-Length Longitudinal Welds

Jen-kan Kent Hsiao
hsiao@engr.siu.edu

Saurav Shrestha

Recommended Citation
Hsiao, Jen-kan K. and Shrestha, Saurav. "Shear Lag Factors for Tension Angles with Unequal-Length Longitudinal Welds." *Advanced Steel Construction* Volume 14, No. 4 (Jan 2019): 589-605. doi:10.18057/IJASC.2018.14.4.

SHEAR LAG FACTORS FOR TENSION ANGLES WITH UNEQUAL-LENGTH LONGITUDINAL WELDS

J. Kent Hsiao[1,*] and Saurav Shrestha[2]

[1]*Professor, Department of Civil and Environmental Engineering, Southern Illinois University Carbondale, Carbondale, IL, USA*
[2]*Former Graduate Student, Department of Civil and Environmental Engineering, Southern Illinois University Carbondale, Carbondale, IL, USA*
[*]*(Corresponding author: Email: hsiao@engr.siu.edu)*

Received: 18 June 2017; Revised: 18 June 2017; Accepted: 19 October 2017

ABSTRACT: When a tension load is transmitted to some, but not all of the cross-sectional elements of a tension member, the tensile force is not uniformly distributed over the cross-sectional area of the tension member. The non-uniform stress distribution in the tension member is commonly referred to as the out-of-plane shear lag effect. The unequal-length longitudinal welds and the in-plane shear lag effect, however, are not addressed by the current American Institute of Steel Construction (AISC) Specification for the determination of the shear lag factors for tension members other than plates and Hollow Structural Sections (HSS). The purpose of this work is to propose a procedure for the computation of shear lag factors accounting for combined in-plane and out-of-plane shear lag effects on unequal-length longitudinal welded angles. The finite element method using three-dimensional solid elements and nonlinear static analyses accounting for combined material and geometric nonlinearities are conducted in this work to verify the accuracy of the proposed procedure.

Keywords: Angle sections, connections, finite element method, geometric nonlinearity, nonlinear analysis, shear lag, stress distribution, welds

DOI: 10.18057/IJASC.2018.14.4

1. INTRODUCTION

The provisions regarding shear lag effects in bolted tension members appeared in the 1978 American Institute of Steel Construction (AISC) Specification (Easterling and Gonzalez [1]; AISC [2]). The 1986 and 1989 AISC Specifications have extended the provisions to welded tension members (AISC [3]; AISC [4]). The 1993 and 1999 AISC Specifications expressed the shear lag provisions using the formula $U = 1 - (\bar{x} / L) \leq 0.9$ for the tension load transmitted only by longitudinal welds to a tension member other than a plate member, where U is the shear lag coefficient, $\bar{x}$ is the connection eccentricity, and L is the length of the connection in the directions of loading (AISC [5]; AISC [6]). The upper limit of 0.9 has been removed in the 2005 and 2010 AISC Specifications (AISC [7]; AISC [8]).

The provisions specified in the current AISC Specification (AISC [8]) only address the out-of-plane shear lag effects for all tension members except plates while the in-plane shear lag effects have been neglected. When a tension load is transmitted to some, but not all of the cross-sectional elements of a tension member other than a plate member, the tensile force is not uniformly distributed over the cross-sectional area of the tension member. The non-uniform stress distribution in the tension member is commonly referred to as the out-of-plane shear lag effect.

Referring to the tension member shown in Figure 1, when the tension load is transmitted to some, but not all of the cross-sectional elements, the effective length of the welded connection is reduced to $L' = L - \bar{x}$, where $\bar{x}$ is the connection eccentricity measured from the plane of the connection to

the member centroid and L is the length of the connection in the direction of loading. Since the reduction in the effective cross-sectional area is proportional to the reduction in the effective connection length, L' / L, the out-of-plane shear lag factor becomes (Geschwindner [9]):

$$U_{OE} = \frac{L'}{L} = \frac{L - \bar{x}}{L} = 1 - \frac{\bar{x}}{L} \tag{1}$$

Therefore, the value of the out-of-plane shear lag factor is influenced by the length of the connection and the geometry of the cross-section of the tension member.

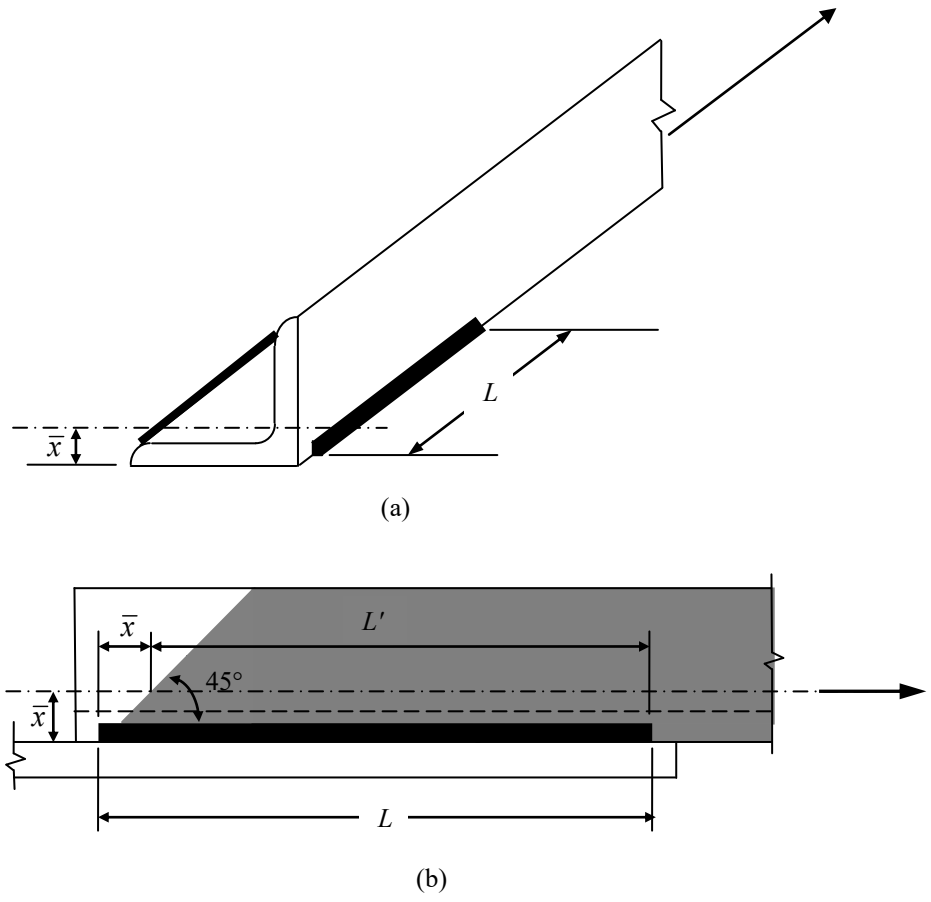

Figure 1. Out-of-Plane Shear Lag Effect on Welded Angle in Tension

In addition to the out-of-plane shear lag effect for unconnected (outstanding) element(s), the in-plane shear lag effect, U_{CE}, for connected element(s) was also recommended to be considered, as given in Eq. (2) (Fortney and Thornton [10]):

$$U_{CE} = \frac{1}{1 + \frac{1}{3}\left(\frac{w}{L}\right)^2} \tag{2}$$

where w = the distance between longitudinal welds and L = the length of weld.

The combined effect of the in-plane and out-of-plane shear lags can be approximately determined as the product of the two component effects as given in Eq. (3) (Fortney and Thornton [10]):

$$U = U_{CE}U_{OE} = \left(\frac{1}{1+\frac{1}{3}\left(\frac{w}{L}\right)^2} \right)\left(1-\frac{\bar{x}}{L}\right) \tag{3}$$

2. NEWLY PROPOSED PROCEDURE FOR THE COMPUTATION OF SHEAR LAG FACTORS

The following addresses a new computation procedure for shear lag factors for tension angles with unequal-length longitudinal fillet welds. Referring to Figure 2, when the width of the welded leg is shorter than the indented distance of the short weld length, [that is, $w \leq (L_1\text{-}L_2)/2$], the out-of-plane shear lag effect on the out-of-plane leg can also be applied to the in-plane leg. Therefore, the in-plane shear lag effect, U_{CE}, for the connected leg can be computed using Eq. (4):

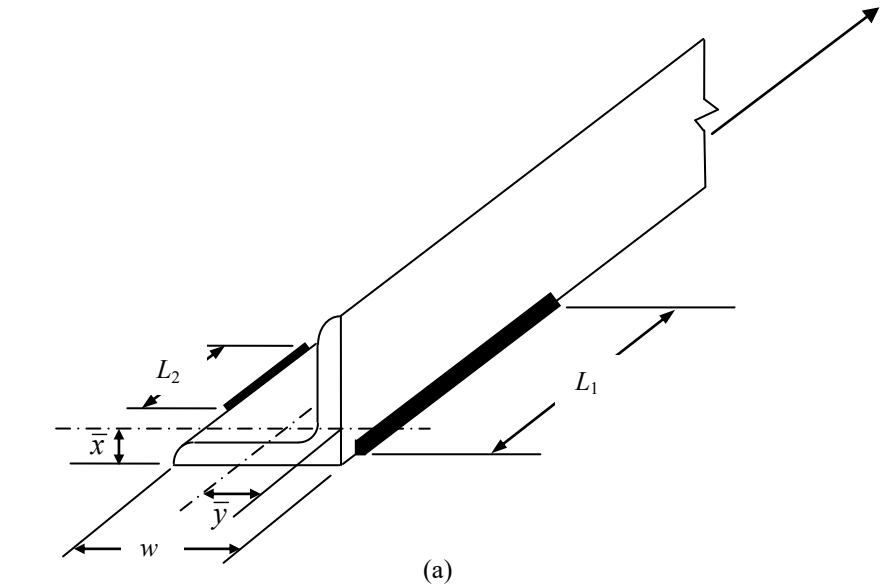

(a)

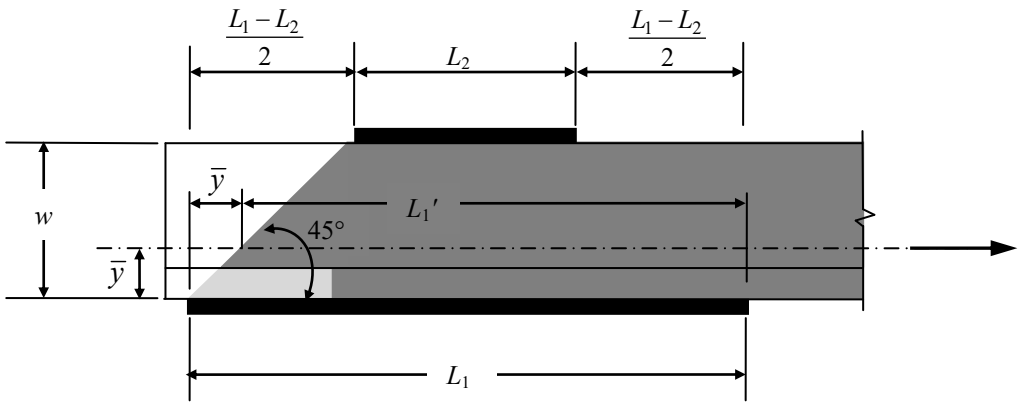

(b)

Figure 2. In-Plane Shear Lag Effect on a Tension Angle with Unequal-Length Welds

$$U_{CE} = \frac{L_1'}{L_1} = \frac{L_1 - \bar{y}}{L_1} = 1 - \frac{\bar{y}}{L_1} \tag{4}$$

The combined effect of the in-plane and out-of-plane shear lags can be approximately determined as the product of the two component effects, as given in Eq. (5):

$$U = U_{CE}U_{OE} = \left(1 - \frac{\bar{y}}{L_1}\right)\left(1 - \frac{\bar{x}}{L_1}\right) \tag{5}$$

where $\bar{x}$ = the distance from the outer face of the connected leg to the centroid of the angle; $\bar{y}$ = the distance from the outer face of the outstanding leg to the centroid of the angle; and L_1 = the length of the longer weld.

3. DESIGN PROCEDURE FOR A TENSION MEMBER TO A GUSSET PLATE CONNECTION

The following are the recommended criteria to be used for the design of a tension member to a gusset plate connection (Astaneh-Asl [11]) using longitudinal fillet welds:

(1) The capacity of the welded connection is recommended to be at least equal to or greater than the axial tension yield capacity of the tension member calculated using a conservative expected yield stress of 1.1 $R_y F_y$ in order to avoid brittle failure of the connections, where R_y is the ratio of the expected yield strength to the specified minimum yield strength of the grade of steel to be used [R_y = 1.5 for ASTM A36 steel channels (AISC [12])] and F_y is the specified minimum yield strength of the grade of steel to be used.

(2) The yielding of the tension member shall occur before the yielding of the gusset plate in order to increase the global ductility of the entire frame:

$$R_y F_y A_g \le F_y A_e \tag{6}$$

where A_g is the cross-sectional area of the tension member and A_e is the area of the Whitmore effective section of the gusset plate.

(3) The design tensile strength for the tensile rupture in the net section of the tension member is recommended to be computed using the following equation (AISC [8]):

$$\phi_t P_n = \phi_t F_u A_n U \tag{7}$$

where $\phi_t = 0.75$; P_n = nominal tensile strength of the tension member; F_u = specified minimum tensile strength of the type of steel being used [F_u = 58 ksi (400 MPa) for ASTM A36 steel]; A_n = net area; and U = shear lag factor.

4. DESIGN EXAMPLE OF THE LONGITUDINAL WELDS BALANCED ABOUT THE NEUTRAL AXIS OF AN ANGLE IN TENSION

Use A36 steel, E70 electrodes to design the longitudinal side fillet welds to develop the full axial yield capacity of a 2L4×3×⅜ LLBB (with long legs back-to-back) tension member connected to a gusset plate. Assume that the tension member is subjected to cyclic loading which results in repeated stress variations; therefore, it is preferable to use two longitudinal welds of unequal length to ensure the welds' centroid will coincide with the centroid of the member so that the transmitted tensile forces will be balanced about the neutral axis of the tension angle (AISC [8]).

4.1 Design of the Unequal-Length Longitudinal Fillet Weld Connection to Balance the Tensile Forces about the Neutral Axis of the Tension Angle

The full axial yield capacity of a L4×3×⅜ tension member can be computed as follows:

$1.1\ R_y\ F_y\ A_g = 1.1\ (1.5)(36\ \text{ksi})(2.49\ \text{in}^2) = 147.9\ \text{kips}\ (658\ \text{kN})$

where $R_y = 1.5$ and $F_y = 36$ ksi (248 MPa) for A36 steel; A_g = the gross area of the tension member.

Assume that the gusset plate is thicker than the angle. In this case, since the material thickness of the thinner part joined is ⅜ in. (10 mm), the minimum weld size = $^3/_{16}$ in. (5 mm) (AISC [8]). Also, since the thickness of the angle is ⅜ in. (10 mm), the maximum weld size = ⅜ - $^1/_{16}$ = $^5/_{16}$ in. (8 mm) (AISC [13]). With the minimum and maximum fillet weld sizes defined, one can use a size of ¼ in. (6 mm) for the fillet weld (since $^3/_{16} \le$ ¼ $\le {}^5/_{16}$, the weld size may be used). The design strength of the weld per inch can thus be computed as follows:

$\phi\ t_e\ (0.60\ F_{EXX}) = 0.75\ [(0.707)\ (¼\ \text{in.})](0.60)(70\ \text{ksi}) = 5.568\ \text{kips/in.}\ (0.975\ \text{kN/mm})$

where t_e = the effective throat of the fillet weld and F_{EXX} = the tensile strength of the weld metal (F_{EXX} =70 ksi for E70 electrodes).

Therefore, the total required weld length can be computed as follows:

$$L_{total} = \frac{147.9\text{kips}}{5.568\text{kips/in.}} = 26.56\ \text{in.}\ (675\ \text{mm})$$

Referring to Figure 3(a), taking the moment about point A to determine the force P_2 and P_1:

$P_2\ (4\ \text{in.}) = (147.9\ \text{kips})\ (1.27\ \text{in.})$

From which, $P_2 = \frac{(147.9)(1.27)}{4} = 47.0$ kips (209 kN), and P_1=147.9 - 47.0 =100.9 kips (449 kN)

Therefore, the required weld length on the outstanding leg side, L_1, and on the flat leg side, L_2, can be computed respectively as follows:

$$L_1 = \frac{100.9}{5.568} = 18.12\ \text{in.} \approx 18.5\ \text{in.}\ (470\ \text{mm})$$

$$L_2 = \frac{47.0}{5.568} = 8.44\ \text{in.} \approx 8.5\ \text{in.}\ (216\ \text{mm})$$

The connection details of the unequal-length longitudinal fillet welds for the angle are shown in Figure 3(b). Note that fillet weld terminations should be located approximately one weld size from the edge of the connection to minimize notches in the base metal (AISC [8]).

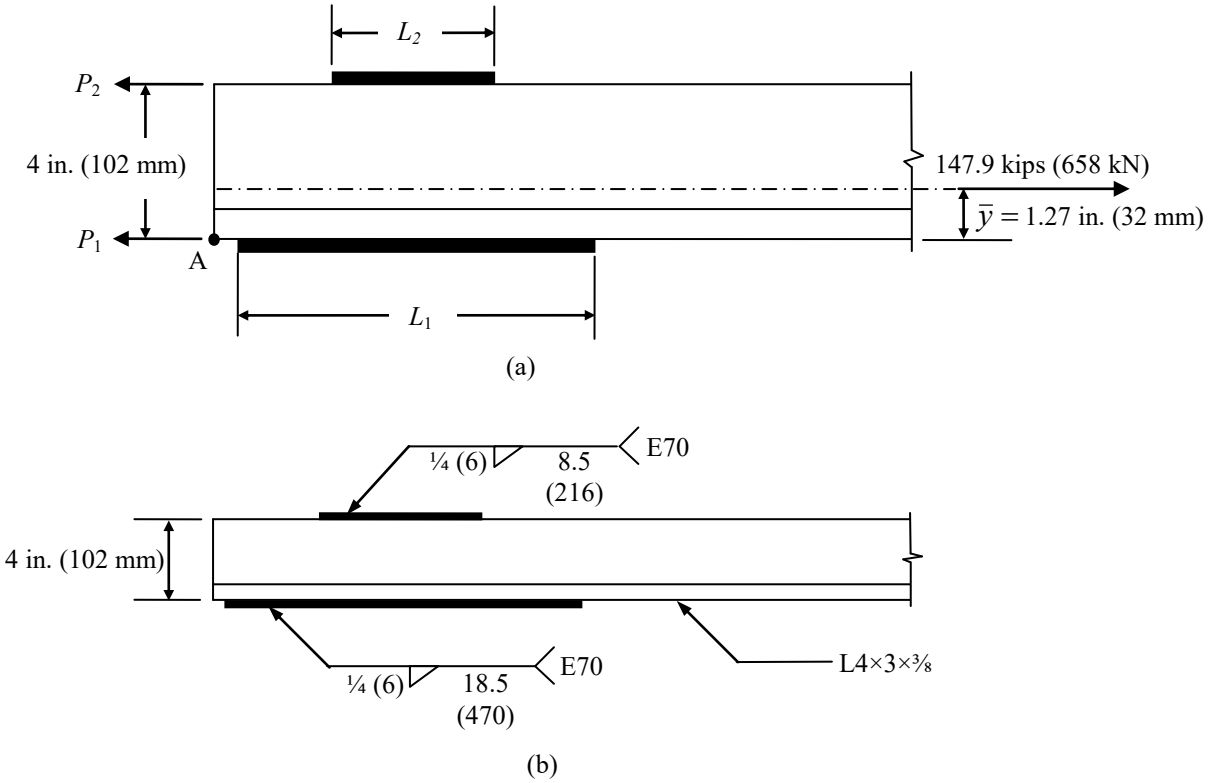

Figure 3. Unequal-Length Longitudinal Fillet Weld Connection for the L4×3×⅜ Tension Member

4.2 Design of the Gusset Plate

Using Eq. (6), one has:

$1.5(36 \text{ ksi})(2)(2.49 \text{ in}^2) \leq (36 \text{ ksi})(A_e)$

From which, the area of the Whitmore effective section, A_e, must be $\geq 7.47 \text{ in}^2$ (4819 mm^2).

Note that in order to avoid the out-of-plane eccentricity effect on the gusset plate (due to one angle being connected to one side of the gusset plate), two L4×3×⅜ angles, with long legs back-to-back, are used as the tension member for this design example.

Referring to Figures 3 and 4, the effective width of the Whitmore section (Whitmore [14]) can be computed to be:

$l_w = (8.5 \text{ in.})(\tan 30°) + (18.5 \text{ in.})(\tan 30°) + 4 \text{ in.} = 19.59 \text{ in. (498 mm)}$

From which, the required thickness of the gusset plate can be computed to be:

$$t = \frac{A_e}{l_w} = \frac{7.47}{19.59} = 0.381 \text{ in. [use } {}^{7}/_{16} \text{ in. (11 mm)]}$$

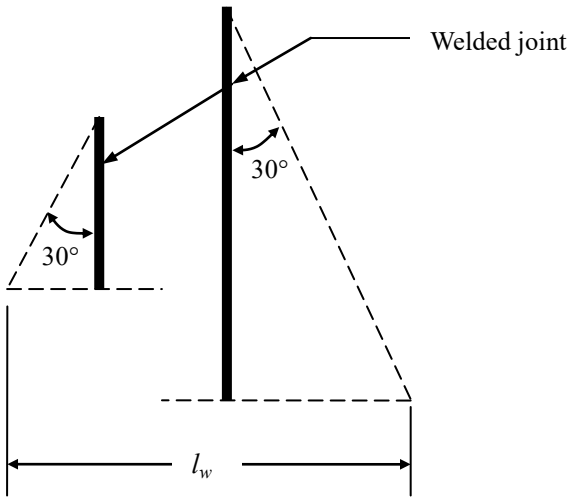

Figure 4. The Whitmore Section for Unequal-Length Welded Joints

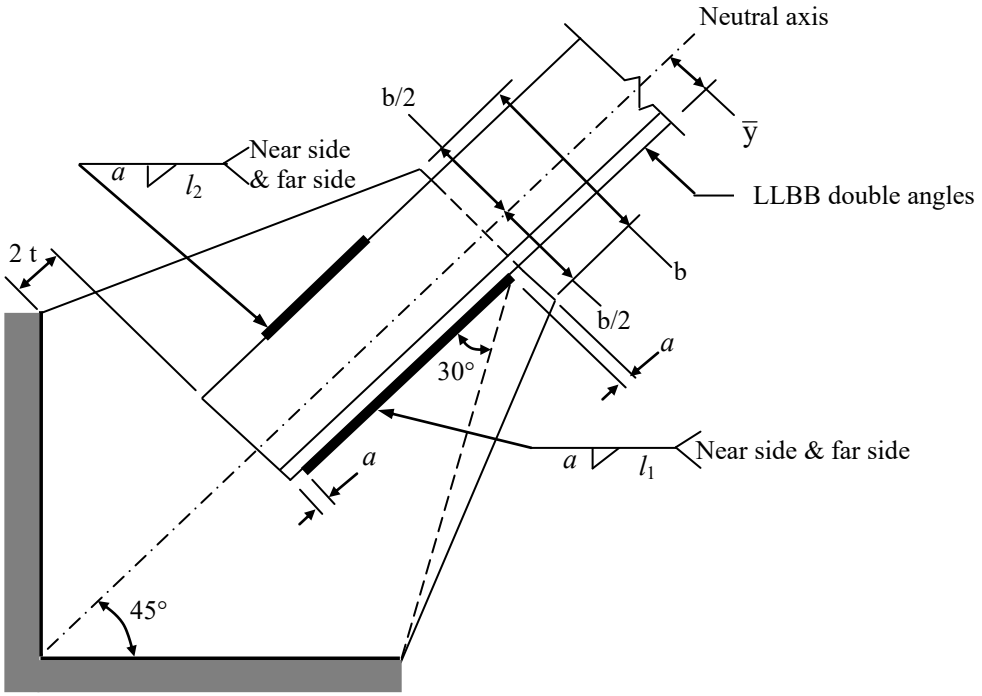

Notes: t = Plate thickness; a = Weld size; l_1 = Long weld length; and l_2 = Short weld length

LLBB Double Angles	$\bar{y}$ in. (mm)	b in. (mm)	t in. (mm)	a in. (mm)	l_1 in. (mm)	l_2 in. (mm)
2L4×3×$^3/_8$	1.27 (32)	6 (152)	$^7/_{16}$ (11)	¼ (6)	18.5 (470)	8.5 (216)
2L6×3½×$^3/_8$	2.02 (51)	8 (203)	$^7/_{16}$ (11)	¼ (6)	24.5 (622)	12.5 (318)
2L6×4×$^9/_{16}$	2 (51)	8 (203)	⅝ (16)	⅜ (10)	25.5 (648)	13 (330)

Figure 5. Unequal-Length Longitudinal Fillet Weld Connection Details for Double Angles

Following the procedure of this design example, the unequal-length longitudinal fillet weld connections for two additional double angles of different sizes (2L6×3½×$^3/_8$ and 2L6×4×$^9/_{16}$) are designed and summarized in Figure 5. Note that in order to ensure that the gusset plate can freely rotate when the double angles are subjected to compression forces, the distance from the end of the double angles to the line that connects the two re-entrant corners of the gusset plate is at least two times the thickness of the gusset plate (Astaneh-Asl [11]).

5. COMPUTATION OF SHEAR LAG FACTORS FOR TENSION ANGLES WITH UNEQUAL-LENGTH LONGITUDINAL FILLET WELD CONNECTIONS

5.1 The AISC Procedure

Since the unequal-length longitudinal welds and the in-plane shear lag effect are not addressed by the current AISC Specification (AISC [8]) for the determination of shear lag factors for tension members other than plates and Hollow Structural Sections (HSS), the following formula may be used for the computation of the U value for the given example, 2L4×3×$^3/_8$, shown in Figure 3.

$$U_{AISC} = U_{OE} = 1 - \frac{\bar{x}}{L}$$

The above formula results in three different U values, depending upon which of the follow three L values are used for this formula:

(1) For $L = l_1$, $U_{AISC(l_1)} = 1 - \dfrac{\bar{x}}{l_1} = 1 - \dfrac{0.775}{18.5} = 0.96$

(2) For $L = \dfrac{l_1 + l_2}{2}$, $U_{AISC(avg)} = 1 - \dfrac{\bar{x}}{\left(\dfrac{l_1 + l_2}{2}\right)} = 1 - \dfrac{0.775}{13.5} = 0.94$

(3) For $L = l_2$, $U_{AISC(l_2)} = 1 - \dfrac{\bar{x}}{l_2} = 1 - \dfrac{0.775}{8.5} = 0.91$

Following the same procedure, the U values for two additional double angles of different sizes (2L6×3½×$^3/_8$ and 2L6×4×$^9/_{16}$ shown in Figure 5) are computed. All the results are summarized in Table 1.

5.2 The Fortney and Thornton Procedure

Fortney and Thornton [10] recommended that Eq. (3) be used for the computation of the U values for angles with unequal-length longitudinal welds. Also, $L = (l_1+l_2)/2$ was recommended to be used for this formula. Using Eq. (3), the U value of the given example, 2L4×3×$^3/_8$, shown in Figure 3, can be computed to be:

$$U_{F\&T} = \left(\frac{1}{1+\frac{1}{3}\left(\frac{w}{\left(\frac{l_1+l_2}{2} \right)} \right)^2} \right) \left(1-\frac{\bar{x}}{\left(\frac{l_1+l_2}{2} \right)} \right) = \left(\frac{1}{1+\frac{1}{3}\left(\frac{4}{13.5} \right)^2} \right) \left(1-\frac{0.775}{13.5} \right) = 0.92$$

Following the same procedure, the U values for two additional double angles of different sizes (2L6×3½×$^3/_8$ and 2L6×4×$^9/_{16}$ shown in Figure 5) are computed. All the results are summarized in Table 2.

5.3 The New Procedure Proposed in this Paper

Eq. (5) is the newly proposed procedure that may also be used for the computation of the U values for angles with unequal-length longitudinal welds. Using Eq. (5), the U value of the given example, 2L4×3×$^3/_8$, shown in Figure 3 [in which w = 4 in. ≤ (L_1-L_2)/2 = 5 in.] can be computed to be:

$$U_{New} = U_{CE}U_{OE} = \left(1-\frac{\bar{y}}{l_1} \right) \left(1-\frac{\bar{x}}{l_1} \right) = \left(1-\frac{1.27}{18.5} \right) \left(1-\frac{0.775}{18.5} \right) = 0.89$$

Since both two additional double angles (2L6×3½×$^3/_8$ and 2L6×4×$^9/_{16}$) shown in Figure 5 satisfy the condition of $w \le (L_1\text{-}L_2)/2$, the U values for both of them can be computed using Eq. (5). The results are summarized in Table 3.

Table 1. Shear Lag Factors Derived from the AISC Specification

$U_{AISC} = U_{OE} = 1-\frac{\bar{x}}{L}$			
LLBB Double Angles	2L4×3×$^3/_8$	2L6×3½×$^3/_8$	2L6×4×$^9/_{16}$
Shear lag factors $U_{AISC(l_1)}$	0.96	0.97	0.96
Shear lag factors $U_{AISC(avg)}$	0.94	0.96	0.95
Shear lag factors $U_{AISC(l_2)}$	0.91	0.94	0.92

Notes: $L = l_1$ for the computation of $U_{AISC(l_1)}$

$L = \frac{l_1+l_2}{2}$ for the computation of $U_{AISC(avg)}$

$L = l_2$ for the computation of $U_{AISC(l_2)}$

Table 2. Shear Lag Factors Derived from Fortney and Thornton

$U_{F\&T} = U_{CE}U_{OE} = \left(\frac{1}{1+\frac{1}{3}\left(\frac{w}{L}\right)^2}\right)\left(1-\frac{\bar{x}}{L}\right)$			
LLBB Double Angles	2L4×3×$^3/_8$	2L6×3½×$^3/_8$	2L6×4×$^9/_{16}$
Shear lag factors $U_{F\&T}$	0.92	0.93	0.92

Note: $L = \frac{l_1 + l_2}{2}$ for the computation of $U_{F\&T}$

Table 3. Shear Lag Factors Derived from the Newly Proposed Formula

$U_{New} = U_{CE}U_{OE} = \left(1-\frac{\bar{y}}{l_1}\right)\left(1-\frac{\bar{x}}{l_1}\right)$			
LLBB Double Angles	2L4×3×$^3/_8$	2L6×3½×$^3/_8$	2L6×4×$^9/_{16}$
Shear lag factors U_{New}	0.89	0.89	0.89

6. COMPUTATION OF SHEAR LAG FACTORS USING THE FINITE ELEMENT METHOD

The finite element method using three-dimensional solid elements and nonlinear static analyses accounting for combined material and geometric nonlinearities are conducted in this work to verify the accuracy of the newly proposed procedure. Figure 6 illustrates the typical length of the tension angles and the applied tensile stress to be used for the construction of the computer models for the finite element analyses using the computer software NISA (NISA [15]).

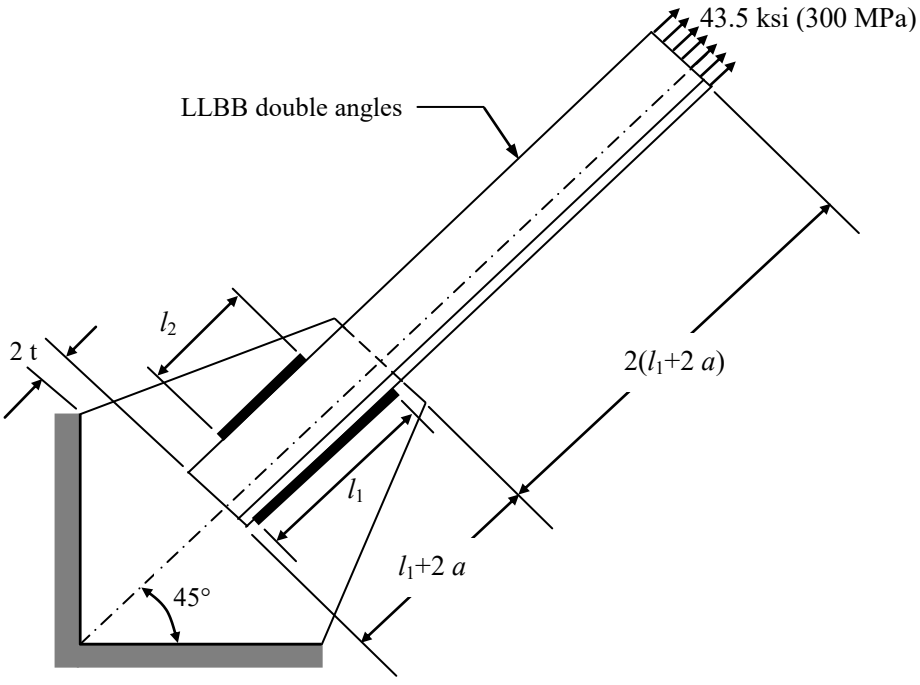

Notes: t = Plate thickness; a = Weld size; l_1 = Long weld length; and l_2 = Short weld length

Figure 6. Typical Length of the Tension Angles and the Applied Tensile Stress at the 100th Time Step

The computer models for the finite element analyses are composed of numerous 8-node hexahedron and 6-node wedge elements. The material properties of the tension angles are: Modulus of elasticity = 29×10^6 psi (200,000 MPa) and Poisson's ratio = 0.3. The analyses account for material nonlinearities based on the elastic, piecewise linear hardening true stress-strain curve, as shown in Figure 7 (derived from Salmon and Johnson [16]) for the A36 steel for tension angles and the elastic, linear hardening, true stress-strain, as shown in Figure 8 (derived from the Lincoln Electric Company [17]) for the E7018 electrode for the longitudinal fillet welds. Therefore, the true stress of 68.73 ksi (474 MPa) and its corresponding strain of 0.1697, as shown in Figure 7, are derived from the engineering stress of 58 ksi (400 MPa) (which is the ultimate tensile stress of A36 steel) and its corresponding strain of 0.185.

A pseudo time of 100 has been used for the time span, which is equivalent to load increments or steps from zero to $\phi_t F_u$. Note that F_u is the ultimate tensile stress of the tension member. Also note that since the first-principal stress is related to fracturing (Cook and Young [18]), there is a critical time step at which the true maximum first-principal stress in the tension angles is closest to 68.73 ksi (474 MPa) (the true ultimate tensile stress). Assuming the i^{th} time step is the critical time step, the allowable applied tensile load at the free end of the tension angles can thus be determined as follows:

$$\text{Allowable applied tensile load} = \phi_t(F_u)(A_g)\,[(i^{th}\text{ time step})/(100\text{ time steps})] \quad (8)$$

Note that $\phi_t F_u = 0.75\times58$ ksi = 43.5 ksi (300 MPa) for A36 steel is used as the applied tensile stress at the 100^{th} time step as shown in Figure 6. Also, A_g is the gross area of the cross-section of the tension member.

Since $A_n = A_g$ for welded tension members, Eq. (9) is then derived from Eqs. (7) and (8):

$$U = (i^{th}\text{ time step})/(100\text{ time steps}) \quad (9)$$

where U is the shear lag factor and the i^{th} time step is the critical time step.

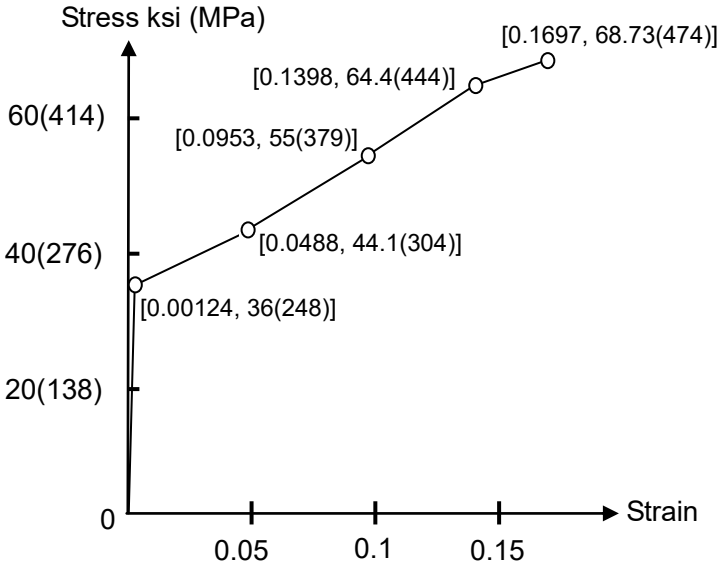

Figure 7. Elastic, Piecewise Linear Hardening, True Stress-Strain Curve for ASTM A36 Steel

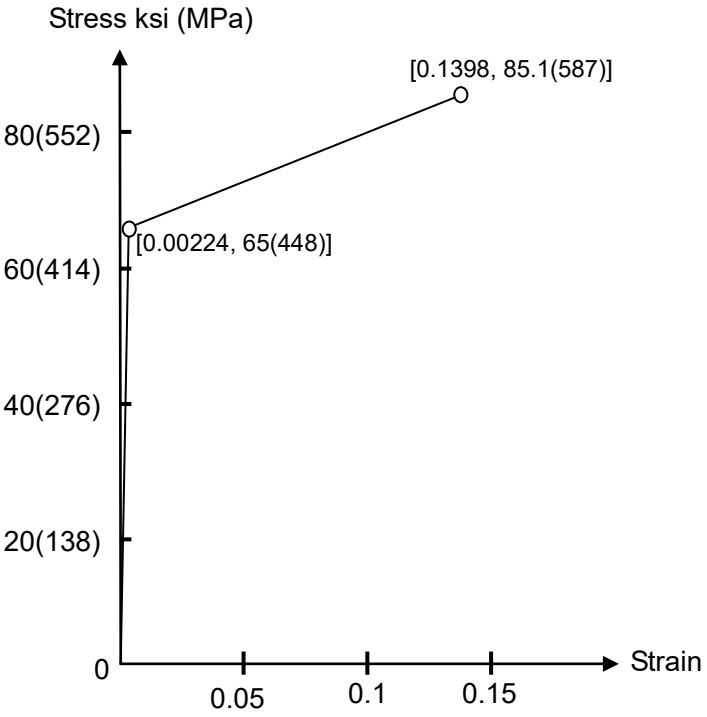

Figure 8. Elastic, Linear Hardening, True Stress-Strain Curve for E7018 Electrode

The results of the finite element analysis for the double angles 2L4×3×$^{3}/_{8}$ are shown in Figures 9, 10, 11, and 12. Figure 9 illustrates that at the 90th time step, the maximum first-principal stress reaches 68.84 ksi (475 MPa) [which is closest to the true ultimate tensile strength of 68.73 ksi (474 MPa)] at the cross-sectional area of the double angles close to the free end of the gusset plate. Therefore, the 90th time step is the critical time step for the 2L4×3×$^{3}/_{8}$ tension member. Furthermore, from Eq. (9), one has U = 90/100 = 0.90 for the 2L4×3×$^{3}/_{8}$ tension member. Figure 10 is a view from the side of the long weld, which illustrates the contour lines of the maximum shear stress distribution at the critical time step for the 2L4×3×$^{3}/_{8}$ tension member. The approximate 45° contour lines of the shear stress distribution at the end of the outstanding leg validate the out-of-plane shear lag effect on the outstanding leg shown in Figure 1. Figure 11 is an overhead view of the contour lines of the maximum shear stress distribution at the critical time step for the 2L4×3×$^{3}/_{8}$ tension member. The approximate 45° contour lines of the shear stress distribution at the end of the connected leg also validate the in-plane shear lag effect on the connected leg shown in Figure 2. Figure 12 illustrates the combined in-plane and out-of-plane shear lag effects on the tension angles.

The results of the finite element analysis for the two additional double angles of different sizes (2L6×3½×$^{3}/_{8}$ and 2L6×4×$^{9}/_{16}$ shown in Figure 5) are shown in Figures 13 and 14, respectively. Both the figures (Figures 13 and 14) illustrate that at the 90th time step, the maximum first-principal stress reaches a critical magnitude [which is closest to the true ultimate tensile strength of 68.73 ksi (474 MPa)] at the cross-sectional area of the double angles close to the free end of the gusset plate. Therefore, the 90th time step is the critical time step for the 2L6×3½×$^{3}/_{8}$ and 2L6×4×$^{9}/_{16}$ tension members. The U values for all the double tension angles determined using the finite element analysis approach are summarized in Table 4.

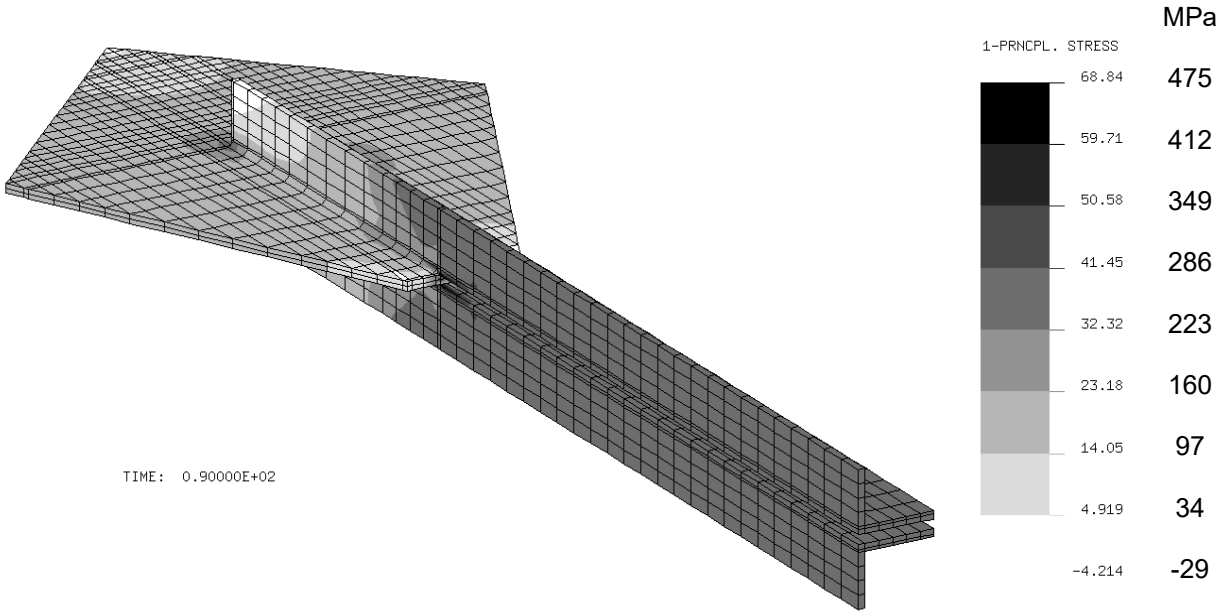

Figure 9. The First-Principal Stress Distribution at the Critical Time Step for the 2L4×3×$^{3}/_{8}$ Tension Member

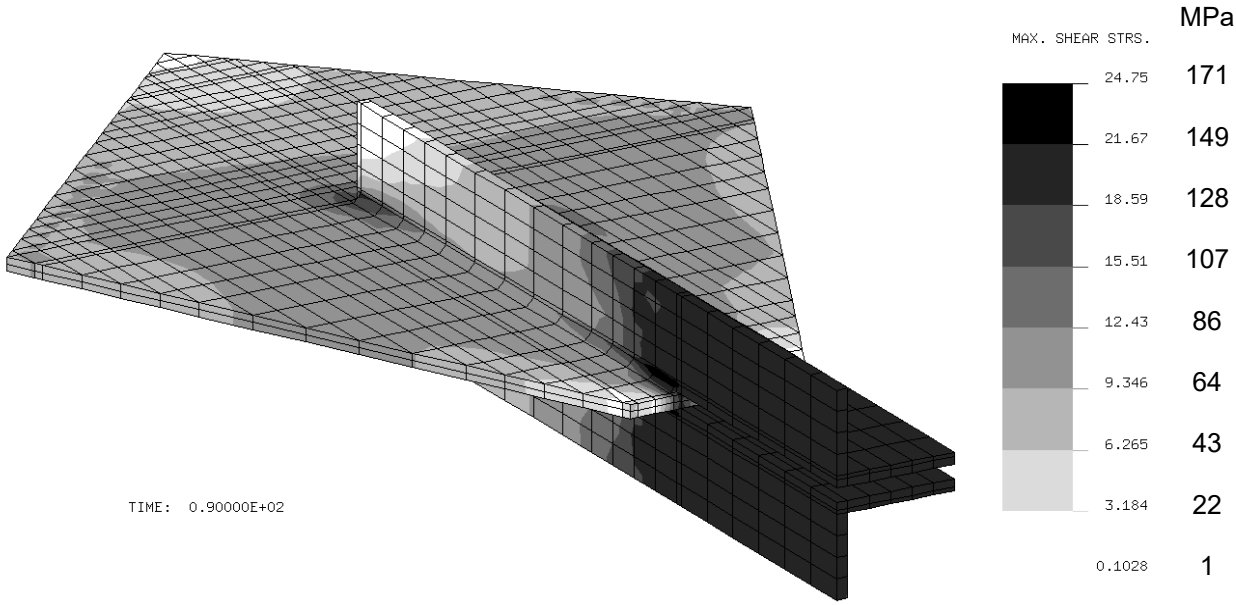

Figure 10. The Maximum Shear Stress Distribution at the Critical Time Step for the 2L4×3×$^{3}/_{8}$ Tension Member (a View from the Side of the Long Weld)

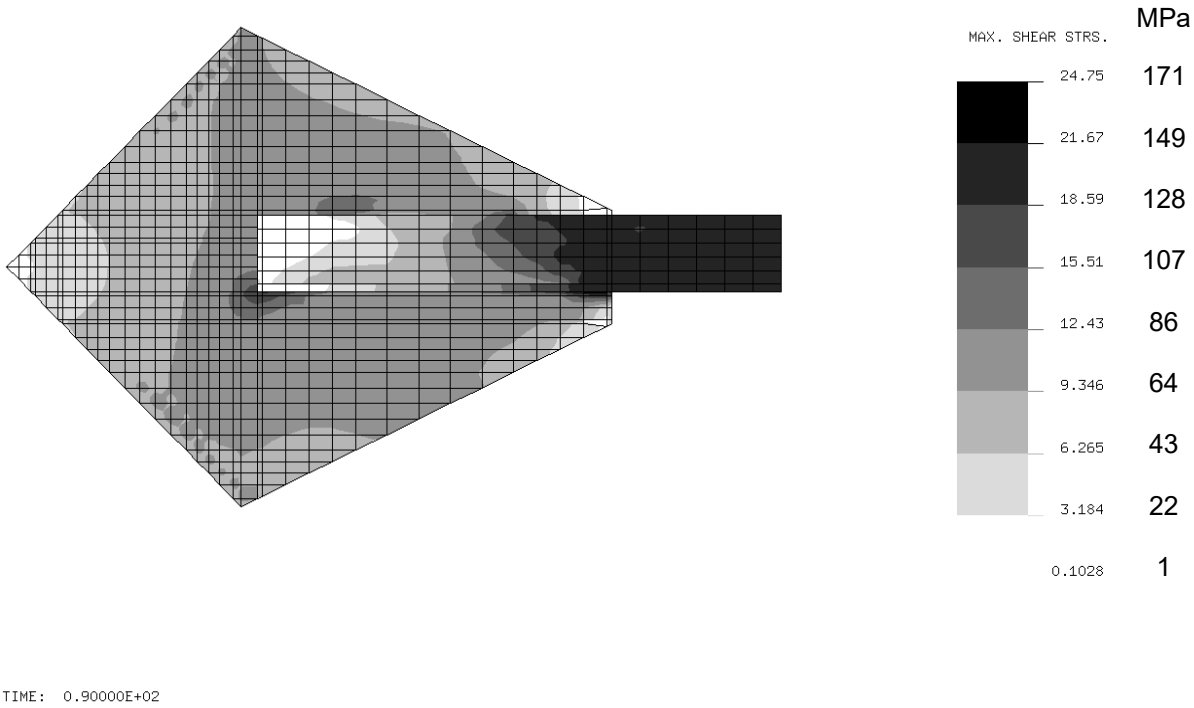

Figure 11. The Maximum Shear Stress Distribution at the Critical Time Step for the 2L4×3×$^{3}/_{8}$ Tension Member (an Overhead View)

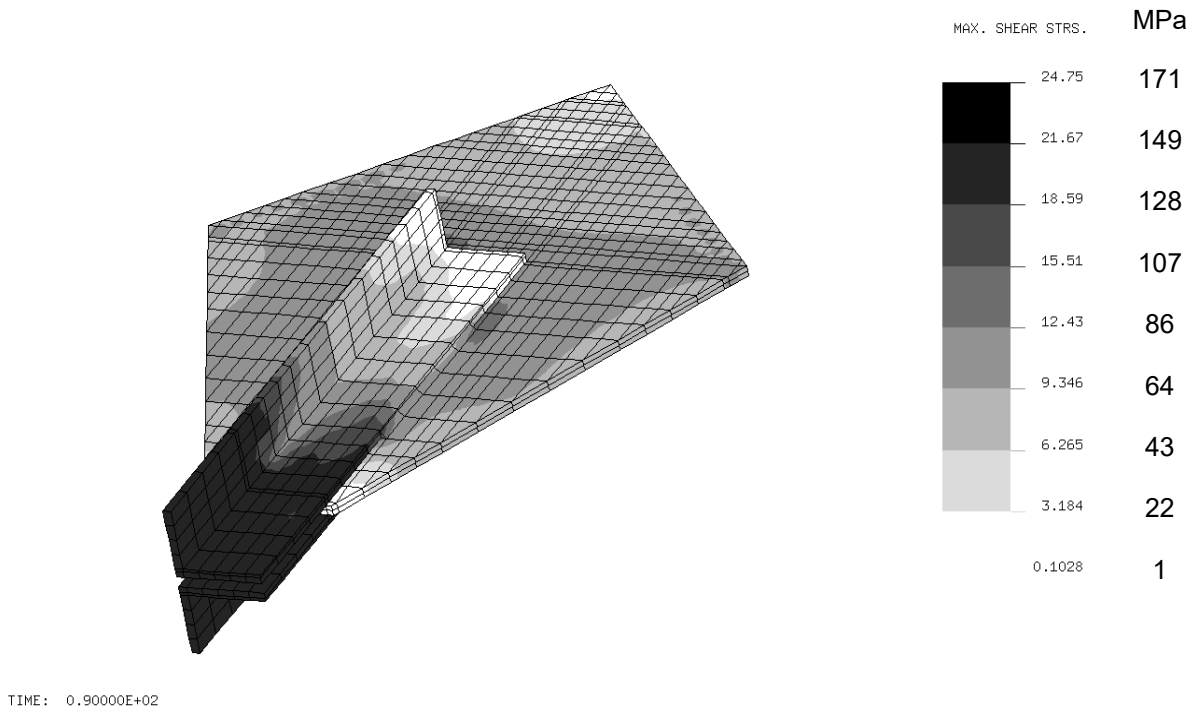

Figure 12. The Maximum Shear Stress Distribution at the Critical Time Step for the 2L4×3×$^{3}/_{8}$ Tension Member (a View from the Side of the Short Weld)

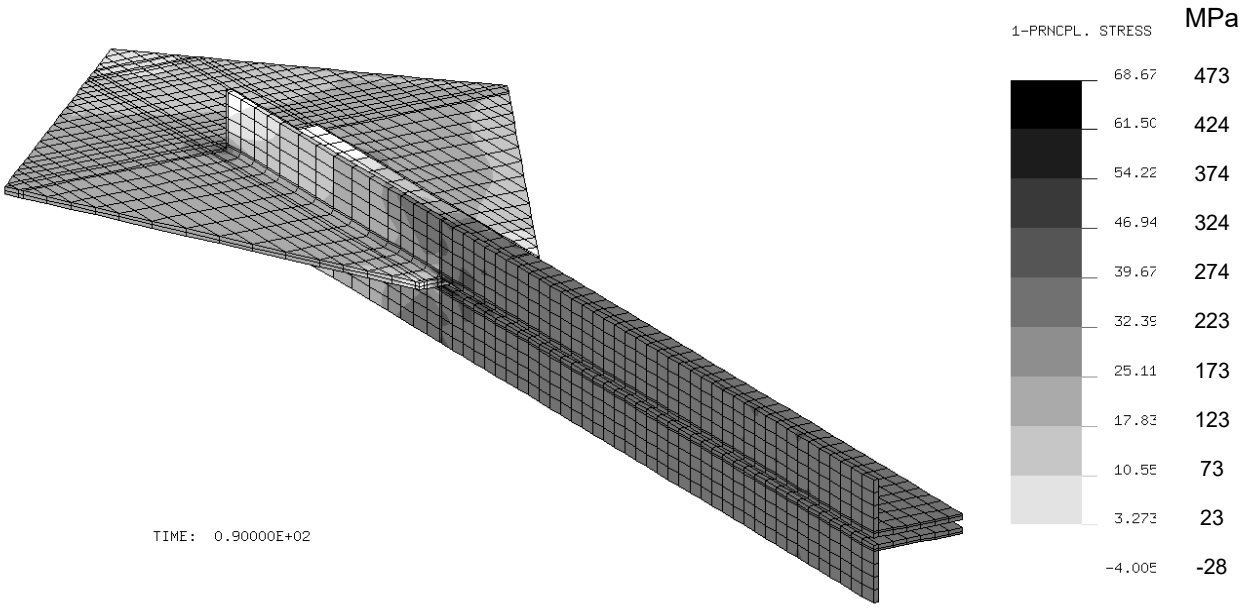

Figure 13. The First-Principal Stress Distribution at the Critical Time Step for the 2L6×3½×$^{3}/_{8}$ Tension Member

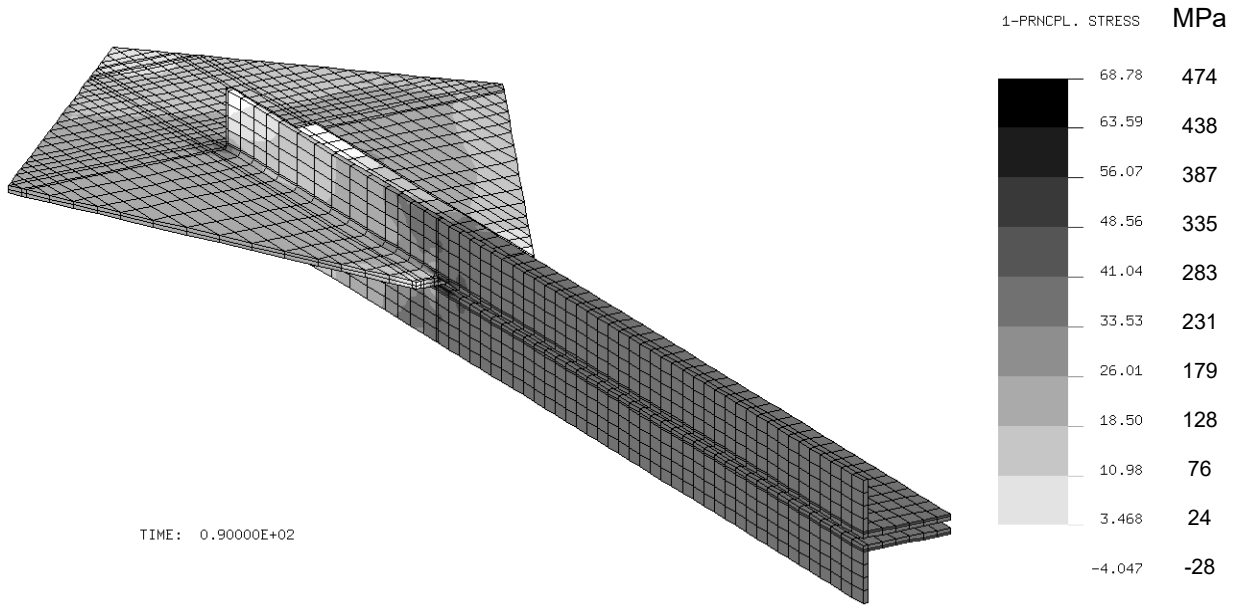

Figure 14. The First-Principal Stress Distribution at the Critical Time Step for the 2L6×4×$^{9}/_{16}$ Tension Member

Table 4. Shear Lag Factors Derived from the Finite Element Analysis Approach

LLBB Double Angles	2L4×3×$^{3}/_{8}$	2L6×3½×$^{3}/_{8}$	2L6×4×$^{9}/_{16}$
Shear lag factors U_{FEA}	0.90	0.90	0.90

A summary of the shear lag factors (U) determined using various approaches is graphically shown in Figure 15. This figure combines the results obtained from Tables 1 through 4. Figure 15 shows that among all the approaches, the newly proposed approach gives the results closest to those obtained using the Finite Element Analysis approach.

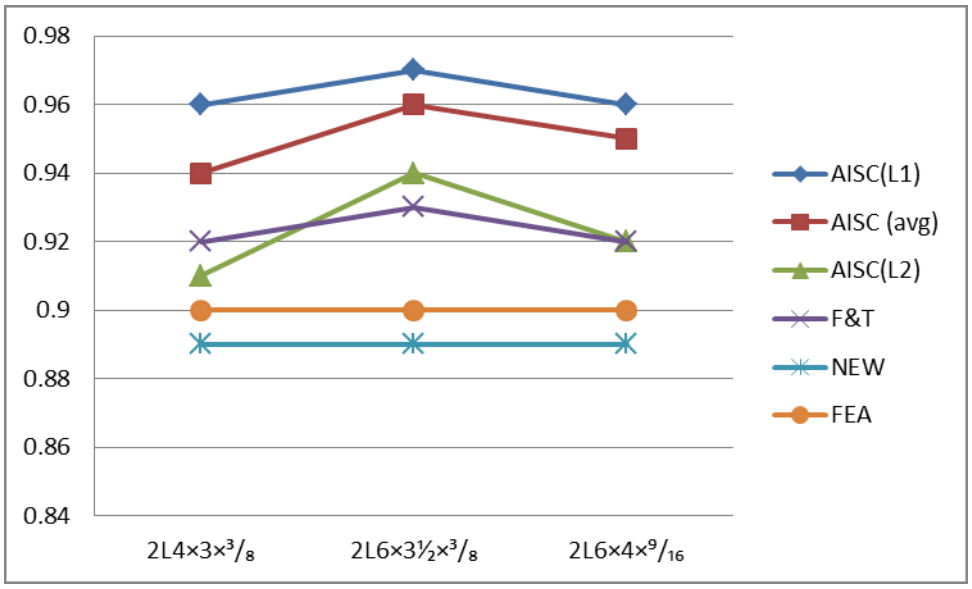

Figure 15. A Summary of the Shear Lag Factors (U) Determined Using Various Approaches

7. CONCLUSIONS

When a tension angle is subjected to cyclic loading, which results in repeated stress variations, it is preferable to use two longitudinal welds of unequal length to ensure the welds' centroid will coincide with the centroid of the angle so that the transmitted tensile forces will be balanced about the neutral axis of the angle. The unequal-length longitudinal welds, however, are not addressed by the current AISC Specification for the determination of the shear lag factor for tension members other than plates and Hollow Structural Sections (HSS). In addition, the current AISC Specification neglects the in-plane shear lag effect for the determination of the shear lag factors for tension members other than plates and HSS. A new procedure for the computation of shear lag factors accounting for combined in-plane and out-of-plane shear lag effects on unequal-length longitudinal welded angles is proposed in this work. The finite element method using three-dimensional solid elements and nonlinear static analyses accounting for combined material and geometric nonlinearities are conducted in this work to verify the accuracy of the proposed procedure. This work concludes that among all the approaches discussed in this paper, the newly proposed approach gives the results closest to those obtained using the Finite Element Analysis approach. However, the newly proposed approach can only be applied when $(l_1\text{-}l_2)/2 \geq w$, where $(l_1\text{-}l_2)/2$ is the indented length at both ends of the short weld, in which l_1 is the length of the long weld and l_2 is the length of the short weld, and w is the width of the in-plane welded leg of the angle.

REFERENCES

[1] Easterling, W.S. and Gonzalez Giroux, L., "Shear Lag Effects in Steel Tension Members", Engineering Journal, American Institute of Steel Construction, 3rd Quarter, 1993, Vol. 30, pp. 77-89.

[2] AISC, "Specification for the Design, Fabrication and Erection of Structural Steel for Buildings", American Institute of Steel Construction, Inc., Chicago, IL., 1978.

[3] AISC, "Specification for Structural Steel Buildings-Load and Resistance Factor Design", American Institute of Steel Construction, Inc., Chicago, IL., 1986.

[4] AISC, "Specification for Structural Steel Buildings-Allowable Stress Design and Plastic Design", American Institute of Steel Construction, Inc., Chicago, IL., 1989.

[5] AISC, "LRFD Specification for Structural Steel Buildings", American Institute of Steel Construction, Inc., Chicago, IL., 1993.

[6] AISC, "LRFD Specification for Structural Steel Buildings", American Institute of Steel Construction, Inc., Chicago, IL., 1999.

[7] AISC, "Specification for Structural Steel Buildings", American Institute of Steel Construction, Inc., Chicago, IL., 2005.

[8] AISC, "Specification for Structural Steel Buildings", American Institute of Steel Construction, Inc., Chicago, IL., 2010.

[9] Geschwindner, L.F., "Unified Design of Steel Structures", John Wiley & Sons, Inc., Upper Hoboken, N.J., 2008.

[10] Fortney, P.J. and Thornton, W.A., "Recommendations for Shear Lag Factors for Longitudinally-Welded Tension Members", Engineering Journal, American Institute of Steel Construction, 1st Quarter, 2012, pp. 11-32.

[11] Astaneh-Asl, A., "Seismic Behavior and Design of Gusset Plates," Steel Tips Report, Structural Steel Educational Council, Moraga, CA., 1998.

[12] AISC, "Seismic Provisions for Structural Steel Buildings", American Institute of Steel Construction, Inc., Chicago, IL., 2005.

[13] AISC, "Steel Construction Manual", 14th Edition, American Institute of Steel Construction, Inc., Chicago, IL., 2011.

[14] Whitmore, R.E., "Experimental Investigation of Stresses in Gusset Plates", Bulletin No. 16, Engineering Experiment Station, Univ. of Tennessee, TN., 1952.

[15] NISA, "NISA User's Manual", the Cranes Software, Inc., Troy, MI, 2005.

[16] Salmon, C.G., Johnson, J.E. and Malhas F.A., "Steel Structures, Design and Behavior", 5th Ed., Pearson Prentice Hall, Upper Saddle River, N.J., 2009.

[17] The Lincoln Electric Company, "The Procedure Handbook of Arc Welding", 13th Ed., The Lincoln Electric Company, Cleveland, OH., 1994.

[18] Cook, R.D. and Young, W.C., "Advanced Mechanics of Materials", Macmillan Publishing Company, New York, N.Y., 1985.